SELF-AERATED FLOWS ON CHUTES AND SPILLWAYS

By H. Chanson[1]

ABSTRACT: In open channel flows, an important design parameter is the amount of entrained air. The presence of air within the flow increases not only the bulk of the flow, but also the transfer of atmospheric gases (e.g. oxygenation). Further aeration of high-velocity flows may prevent or reduce cavitation damage. The present paper reviews the characteristics of self-aerated flows on spillways and chutes, including uniform flows and gradually varied flows. First, the uniform flow conditions are presented with new prototype results. Similarities with suspended-sediment flows and extremely rough flows are developed and the interaction between air bubbles and turbulence is discussed. Then, the basic equations for gradually varied flows are developed using the same method as Wood in 1985. The results are applied to chutes and tunnel spillways and are compared with experimental data.

INTRODUCTION

The presence of air in open channel flows increases the bulk of the flow which must be taken into account when designing spillway and chute sidewalls (Falvey 1980). Also, the presence of air within the boundary layer reduces the shear stress, and the resulting increase of momentum must be considered when designing a ski jump downstream of a spillway (Ackers and Priestley 1985). Further, the presence of air within high-velocity flows may prevent or reduce the damage caused by cavitation (May 1987; Falvey 1990). Air entrainment on chutes has been recognized also for its contribution to the air-water transfer of atmospheric gases such as oxygen and nitrogen (Wilhelms and Gulliver 1989).

In the first part of the present paper, uniform self-aerated flows are studied using the same method used by Wood (1983). Comparisons are made with experimental data. The results are discussed with analogy to flows over rockfill dams and suspended sediments flows. In the second part of the paper, the gradually varied flow region is described using the same method as that used by Wood (1985). The results are discussed and compared with experimental data.

Mechanisms of Air Entrainment on Chutes

In high-speed flow down a steep chute, air is entrained at the free surface; this process is called self aeration. Several explanations were proposed to describe the mechanisms of self aeration. Keulegan and Patterson (1940) analyzed wave instability in open channel flows, and their work suggests that air may be entrained by breaking waves at the free surface, if the flow conditions satisfy $F > 1.5$. Volkart (1980) indicated that air is entrained by water drops falling back into the water flow. Hino (1961) and Ervine and Falvey (1987) suggested that air is entrapped by turbulent velocity fluctuations on the free surface.

[1]Lect., Hydr. and Fluid Mech., Dept. of Civ. Engrg., Univ. of Queensland, St. Lucia QLD 4072, Australia.

It is believed that air entrainment occurs when the turbulence level is large enough to overcome both surface tension and gravity effects. The turbulent velocity normal to the free surface v' must be large enough to overcome the surface tension pressure of the entrained bubble (Rao and Rajaratnam 1961; Ervine and Falvey 1987) and greater than the bubble rise velocity component for the bubble to be carried away. These conditions become

$$v' > \sqrt{\frac{8\sigma}{\rho_w d_b}} \quad \dots\dots\dots\dots\dots\dots\dots\dots\dots\dots\dots\dots\dots (1)$$

$$v' > u_r \cos\alpha \quad \dots\dots\dots\dots\dots\dots\dots\dots\dots\dots\dots\dots\dots\dots (2)$$

where σ = surface tension; ρ_w = water density; d_b = bubble diameter; u_r = bubble rise velocity; α = spillway slope. Air entrainment occurs when the turbulent velocity v' satisfies both (1) and (2). It must be noted that (1) derives from Ervine and Falvey's (1987) work. Fig. 1 shows both conditions for bubble sizes in the range of 1–100 mm and slopes from 0° to 75°. The rise velocity of individual bubbles in still water was computed as by the method of Comolet (1979). Fig. 1 suggests that self aeration will occur for turbulent velocities normal to the free surface greater than 0.1–0.3 m/s and bubbles in the range of 8–40 mm. For steep slopes the action of the buoyancy force is reduced and larger bubbles are expected to be carried away.

Self-Aeration on Spillway Chute

For a spillway flow, the entraining region follows a region where the flow over the spillway is smooth and glassy. Next to the boundary, however, turbulence is generated and the boundary layer grows until the outer edge of the boundary layer reaches the surface. This point is called the point of inception (Fig. 2). Downstream of the point of inception, a layer containing
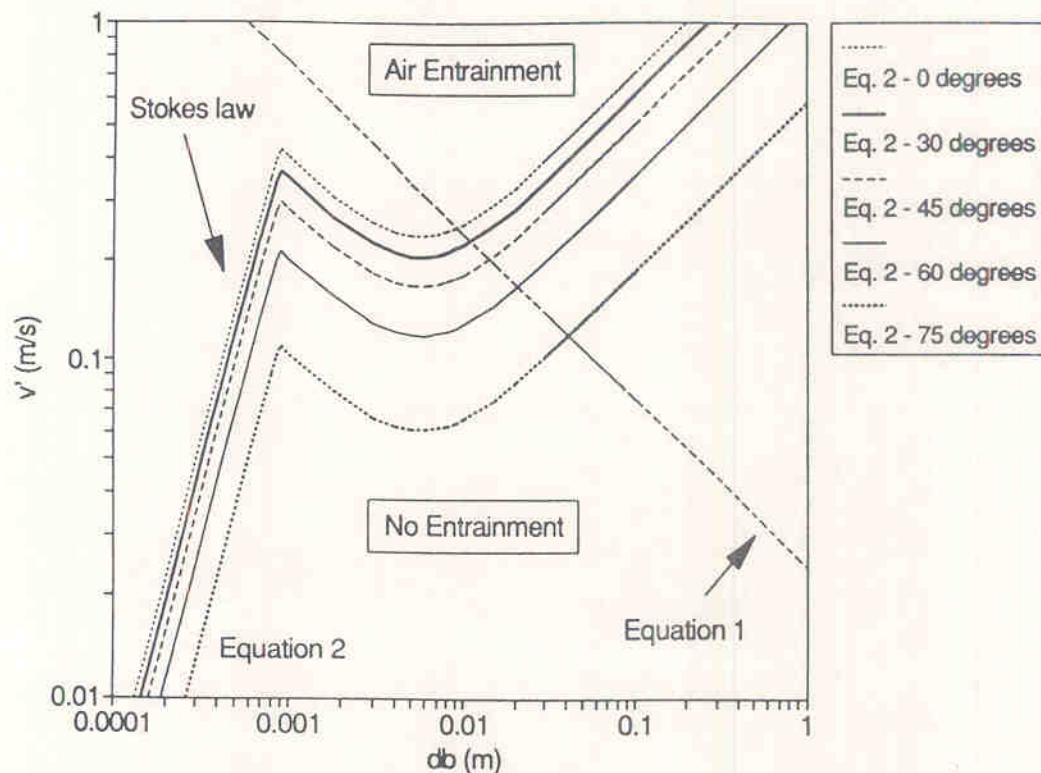

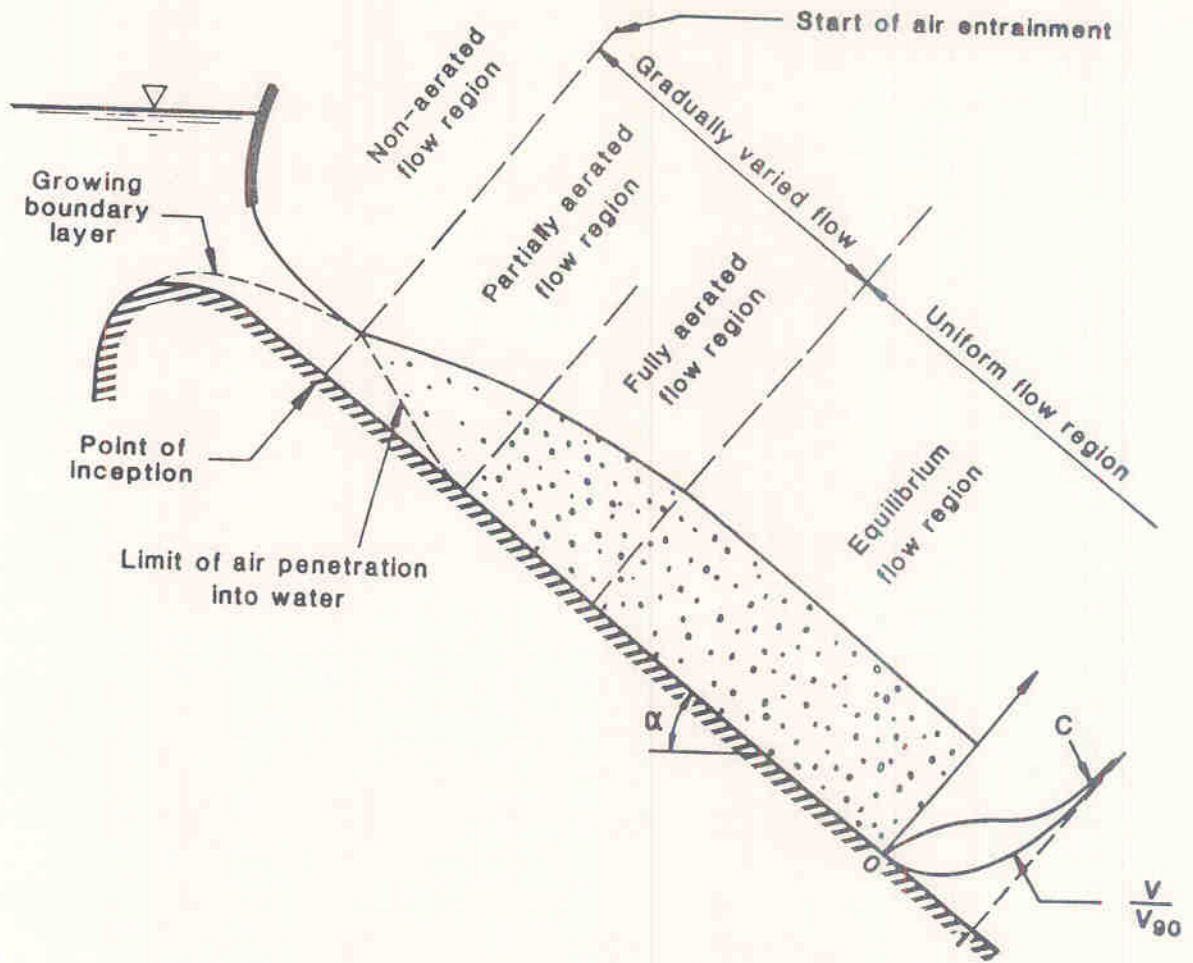**FIG. 1. Critical Turbulent Velocity v' for Air Entrainment**

FIG. 2. Self-Aeration on Chute Spillway

a mixture of both air and water extends gradually through the fluid. The rate of growth of the layer is small and the air concentration distribution varies gradually with distance. Far downstream, the flow will become uniform. This region is defined as the uniform equilibrium flow region.

Definitions

The local air concentration is defined as the volume of air per unit volume. The characteristic flow depth d is defined as

$$d = \int_0^{Y_{90}} (1 - C)\, dy \quad \dots\dots\dots\dots\dots\dots\dots\dots\dots\dots\dots\dots\dots\dots\dots\dots\dots (3)$$

where y is measured perpendicular to the spillway surface; Y_{90} = depth where the local air concentration is 90%. The model and prototype data presented in this paper were obtained using conductivity probes. A conductivity probe records the average time of passage of air bubbles and provides the air concentration only if the air velocity equals the water velocity (i.e. $V_{air}/V_w = 1$). Above 90% of air concentration, the slip ratio V_{air}/V_w no longer equals 1 (Cain 1978, Chanson 1988), and the characteristic depth d must be defined from 0 to 90% only. The depth averaged mean air concentration C_{mean} is defined as

$$(1 - C_{mean})\, Y_{90} = d \quad \dots\dots\dots\dots\dots\dots\dots\dots\dots\dots\dots\dots\dots\dots\dots\dots\dots\dots (4)$$

The average water velocity U_w is defined as

$$U_w = \frac{q_w}{d} \quad \dotsfill (5)$$

where q_w = water discharge per unit width. The characteristic velocity V_{90} is defined as that at Y_{90}.

UNIFORM FLOW REGION

Equilibrium Air Concentration Distribution

Wood (1983) reanalyzed Straub and Anderson's (1958) set of self-aerated flow measurements. The analysis showed that the average air concentration for uniform flow conditions C_e is independent of the upstream geometry (i.e. discharge, Froude number, relative roughness) and is a function of the slope only (Table 1, column 2). Fig. 3 shows the average air concentration C_e as a function of the slope α for Straub and Anderson's (1958) data obtained on a model and field data presented by Aivazyan (1987). The agreement between the model and prototype data is good. For slopes flatter than 50°, the average air concentration may be estimated as

$$C_e = 0.9 \sin \alpha \quad \dotsfill (6)$$

It must be noted that Aivazyan's (1987) and Jevdjevich and Levin's (1953) data were initially presented with reference of the depth Y_{98} corresponding to 98% air concentration and were recalculated with reference to Y_{90}.

Hartung and Scheuerlein (1970) studied open channel flows with large natural roughness (k_s in the range of 0.1–0.35 m) and steep slopes (α in the range of 6°–34°). The extremely rough bottom induced a highly turbulent

TABLE 1. Dimensionless Air Concentration and Velocity Distribution in Uniform Self-Aerated Flow

Slope (degrees) (1)	C_{mean} [a] (2)	$G' \cos \alpha$ [b] (3)	B' [b] (4)	$\dfrac{q_w}{V_{90}Y_{90}}$ (5)	M (6)	E (7)
			(a) Values			
7.5	0.161	8.000	0.003021	0.688	1.029	1.075
15.0	0.241	5.745	0.02880	0.609	1.039	1.097
22.5	0.310	4.834	0.07157	0.554	1.033	1.085
30.0	0.410	3.825	0.19635	0.467	1.042	1.105
37.5	0.569	2.675	0.6203	0.335	1.061	1.148
45.0	0.622	2.401	0.8157	0.301	1.038	1.097
60.0	0.680	1.894	1.354	0.241	1.107	1.249
75.0	0.721	1.574	1.864	0.206	1.138	1.318
(b) Analytical formula for a power law velocity distribution (eq. (10))						
—	—	—	—	$\dfrac{n}{n+1}$	$\dfrac{(n+1)^2}{n(n+2)}$	$\dfrac{(n+1)^3}{n^2(n+3)}$
(c) Computed value for $n = 6.0$						
—	—	—	—	0.857	1.021	1.059

[a] Data from Straub and Anderson (1958).
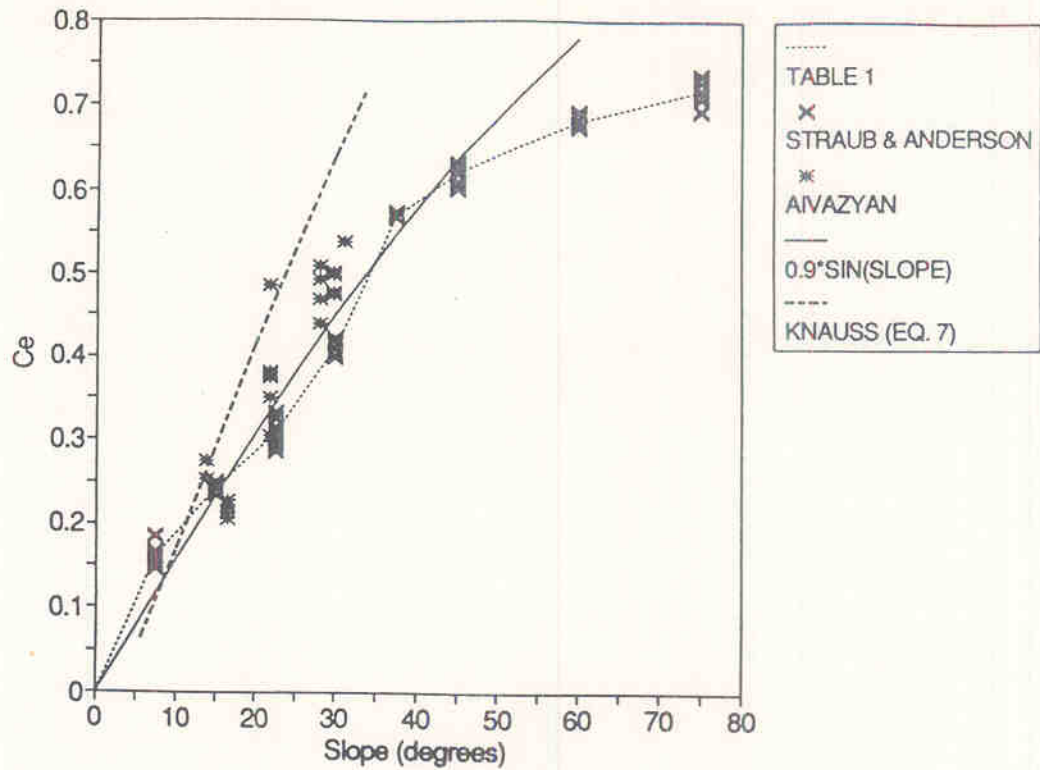[b] Computed from Straub and Anderson's (1958) data.

FIG. 3. Equilibrium Air Concentration as Function of Channel Slope (Straub and Anderson 1958; Aivazyan 1986)

flow with air entrainment. Knauss (1979) indicated that the quantity of air entrained was estimated as

$$C_e = 1.44 \sin \alpha - 0.08 \quad \ldots\ldots\ldots\ldots\ldots\ldots\ldots\ldots\ldots\ldots\ldots\ldots\ldots\ldots\ldots (7)$$

This result is of similar form as (6). Both (6) and (7) are plotted on Fig. 3.

For a given mean air concentration the diffusion of air bubbles within the air-water mixture can be represented by a simple model developed by Wood (1984)

$$C = \frac{B'}{B' + \exp[-(G \cos\alpha \, y'^2]} \quad \ldots\ldots\ldots\ldots\ldots\ldots\ldots\ldots\ldots (8)$$

where B' and G' are functions of C_e only (Table 1, columns 3 and 4); and $y' = y/Y_{90}$. However, next to the spillway surface, Cain's (1978) and Chanson's (1988) data depart from (8), and show consistently that the air concentration tends toward zero at the bottom. A reanalysis of the data indicates the presence of an air concentration boundary layer, in which the air concentration distribution may be estimated as

$$C = k \sqrt[3]{\frac{y}{\delta_{ab}}} \quad \ldots\ldots\ldots\ldots\ldots\ldots\ldots\ldots\ldots\ldots\ldots\ldots\ldots\ldots\ldots\ldots (9)$$

where k is a constant that satisfies the continuity between (8) and (9); and δ_{ab} is the air concentration boundary layer thickness $\delta_{ab} = 10-15$ mm (Chanson 1989).

Velocity Distribution

Measurements of velocity within self-aerated flows were performed on Aviemore dam by Cain (1978), and Cain and Wood (1981) showed that the velocity distribution can be approximated by

$$\frac{V}{V_{90}} = \left(\frac{y}{Y_{90}}\right)^{1/n} \dots \dots \dots \dots \dots \dots \dots \dots \dots \dots \dots \dots \dots \dots (10)$$

where the exponent $n = 6.00$ (Chanson 1989) for the roughness of the Aviemore dam [$k_s = 1$ mm (Cain 1978)]. For uniform nonaerated flows, Chen (1990) derived a theoretical relation between the exponent n and the friction factor f as

$$n = K \sqrt{\frac{8}{f}} \dots \dots \dots \dots \dots \dots \dots \dots \dots \dots \dots \dots \dots \dots \dots \dots (11)$$

where K = Von Karman universal constant ($K = 0.4$); and f is dependent upon the Reynolds number and the roughness. On Aviemore dam, (11) would imply $f = 0.0356$, which is higher than the values computed from the Colebrook-White formula for nonaerated flow (i.e. $f = 0.023$ and 0.022).

Cain's (1978) measurements were made in the gradually varied flow region with the mean air concentration in the range of 0–50%. To a first approximation, the dimensionless velocity distribution V/V_{90} is independent of the air concentration. It is reasonable to believe that this also applies in the uniform flow region (Wood 1985). The characteristic velocity V_{90} may be deduced by combining (10) with the continuity equation for the water phase, and this yields

$$\frac{q_w}{Y_{90}V_{90}} = \int_0^1 (1 - C)y'^{1/n} \, dy' \dots \dots \dots \dots \dots \dots \dots \dots (12)$$

where C is computed from (8). For the air-water mixture, it is also possible to define a momentum correction parameter M and a kinetic energy parameter E as

$$M = \frac{\displaystyle\int_0^{Y_{90}} (1 - C)V^2 \, dy}{\displaystyle\frac{1}{d}\left[\int_0^{Y_{90}} (1 - C)V \, dy\right]^2} \dots \dots \dots \dots \dots \dots \dots \dots (13)$$

$$E = \frac{\displaystyle\int_0^{Y_{90}} (1 - C)V^3 \, dy}{\displaystyle\frac{1}{d^2}\left[\int_0^{Y_{90}} (1 - C)V \, dy\right]^3} \dots \dots \dots \dots \dots \dots \dots \dots (14)$$

where d is defined in (3). Using (10), the dimensionless formulation of these parameters becomes

$$M = (1 - C_e) \frac{\displaystyle\int_0^1 (1 - C)y'^{2/n} \, dy'}{\left(\displaystyle\int_0^1 (1 - C)y'^{1/n} \, dy'\right)^2} \dots \dots \dots \dots \dots \dots (15)$$

$$E = (1 - C_e)^2 \frac{\displaystyle\int_0^1 (1 - C)y'^{3/n} \, dy'}{\left[\displaystyle\int_0^1 (1 - C)y'^{1/n} \, dy'\right]^3} \dots \dots \dots \dots \dots \dots (16)$$

Eqs. (12), (15), and (16) provide the analytical solutions for V_{90}, M, and E. For $n = 6.0$, they are plotted in Figs. 4 and 5 as a function of the average air concentration and compared with experimental data obtained on prototype (Jevdjevich and Levin 1953; Cain 1978) and model (Chanson 1988).
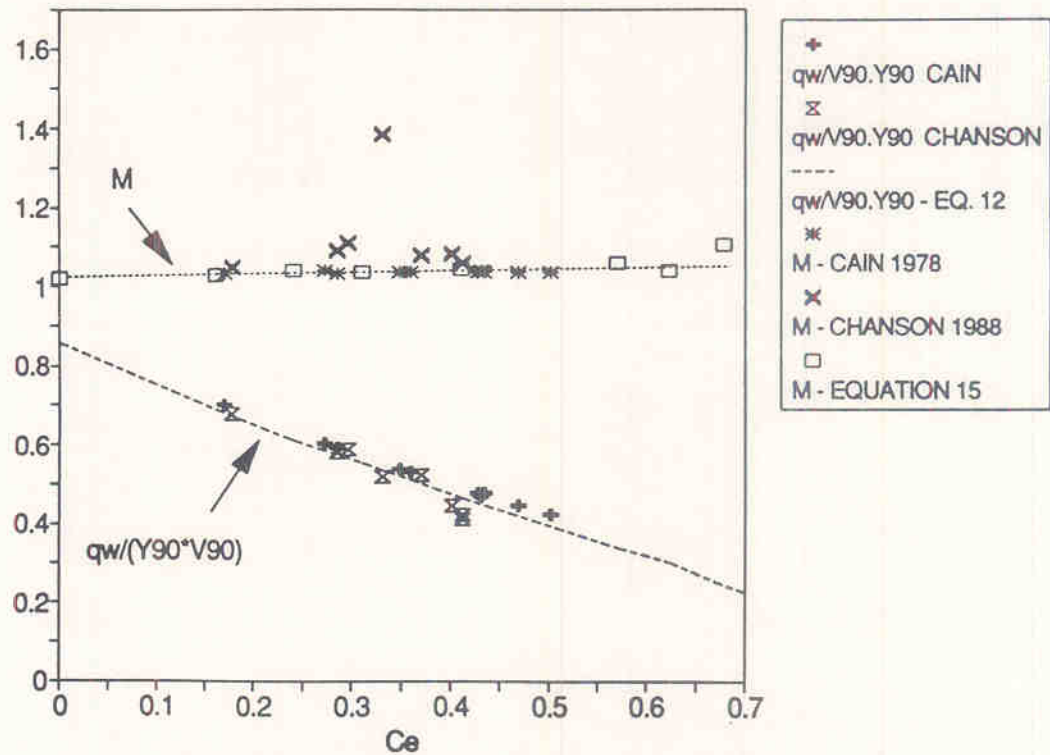

FIG. 4. Characteristic Velocity V_{90} and Momentum Correction Coefficient M as Function of Equilibrium Air Concentration C_e
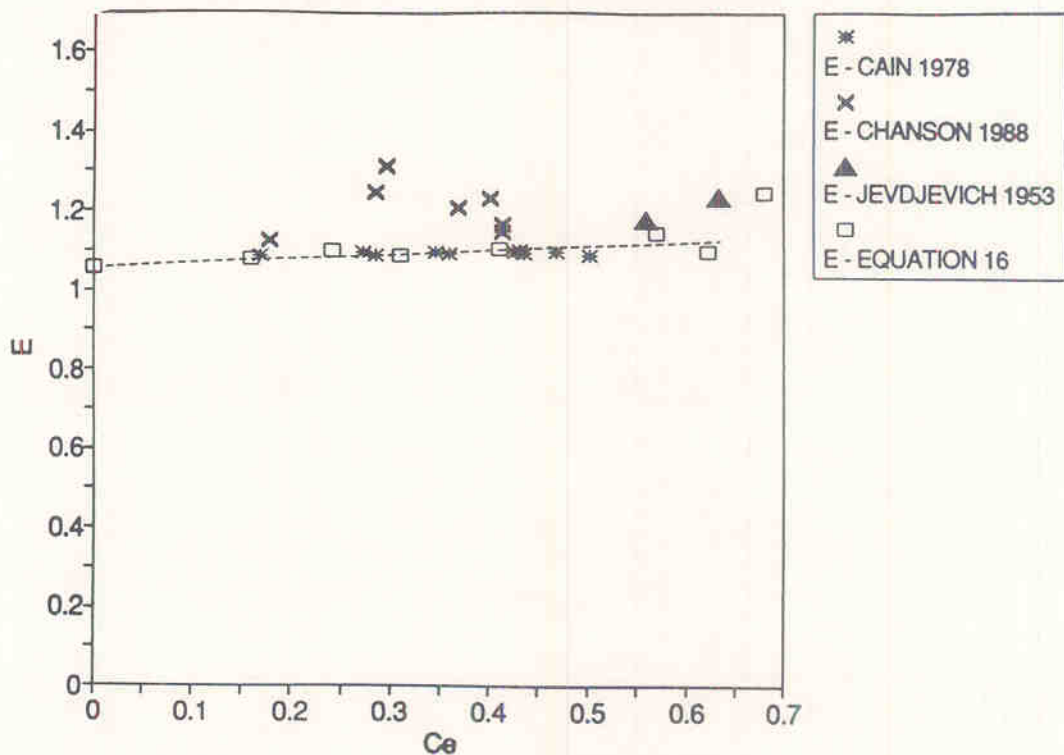

FIG. 5. Kinetic Energy Correction Coefficient E as Function of Equilibrium Air Concentration C_e

The scatter of the model data differs from the prototype results because of the limitation of the instrumentation on the spillway model.

Friction Factor of Self-Aerated Flows

For uniform aerated flow the energy equation yields

$$f_e = \frac{8g \sin \alpha \, d^2}{q_w^2} \left(\frac{D_H}{4} \right) \quad \dotfill \quad (17)$$

where f_e = friction factor for the uniform air-water mixture; and D_H = the hydraulic diameter. Wood (1983) analyzed Straub and Anderson's (1958) data and showed that the friction factor for aerated flow f_e decreases when the average air concentration increases. Prototype data (Jevdjevich and Levin 1953; Aivazyan 1987) confirmed the reduction in the friction factor observed on model. The data were reanalyzed using (17) formulated in terms of hydraulic diameters to take into account the shape of the channel cross section. The results are presented in Fig. 6 where the ratio f_e/f is plotted as a function of the average air concentration, f being the nonaerated friction factor calculated using the Colebrook-White formula. Details of the range of roughness and Reynolds numbers are reported in Table 2.

Dimensional analysis suggests that the ratio f_e/f is a function of the average air concentration, Reynolds number, and roughness

$$\frac{f_e}{f} = \Phi \left(C_e; \ \mathsf{R}; \ \frac{k_s}{D_H} \right) \quad \dotfill \quad (18)$$

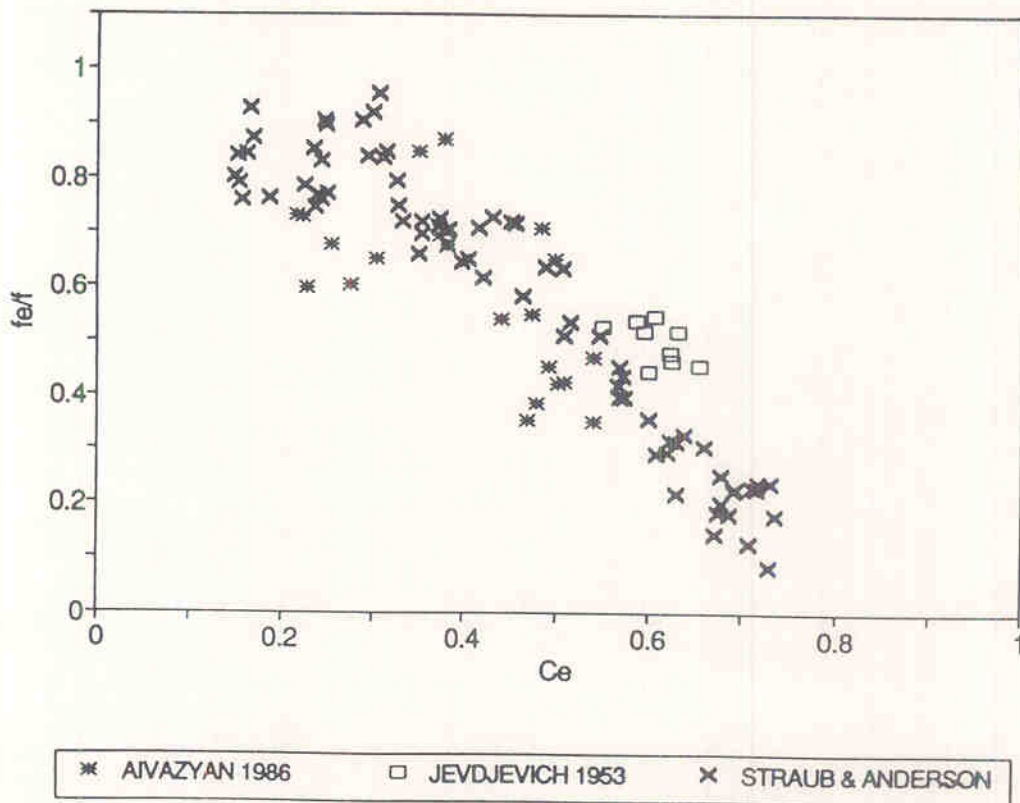The writer investigated the effect of the Reynolds number and the rough-

FIG. 6. Relative Friction Factor f_e/f as Function of Equilibrium Air Concentration C_e

TABLE 2. Flow Conditions for Jevdjevich and Levin (1953), Straub and Anderson (1958), and Aivazyan (1987)

Experiment (reference) (1)	Slope (degrees) (2)	k_S (mm) (3)	k_S/D_H (4)	R (5)	C_{mean} (6)	Comments (7)
Mostarsko Blato; (Jevdjevich and Levin 1953)	—	10 to 20	0.015 to 0.035	$8.3E + 4$ to $3E + 7$	0.58 to 0.66	Prototype; wide channel ($W = 5.75$ m); stone lining.
(Straub and Anderson 1958)	7.5 to 75	0.71	3E-3 to 1.6E-2	$4.7E + 5$ to $2E + 6$	0.15 to 0.73	Spillway model ($W = 0.457$ m); artificial roughness.
(Aivazyan 1987)	14 to 31	0.1 to 10	5E-4 to 0.04	$1.7E + 5$ to $2.8E + 7$	0.21 to 0.54	Prototype and large spillway model ($W = 0.25$ to 6 m); planed boards, wood, rough concrete, and rough stone masonry.

ness on the ratio f_e/f. For the data of Jevdjevich and Levin (1953), Straub and Anderson (1958), and Aivazyan (1987), (18) is estimated by (Appendix I)

$$\frac{f_e}{f} = 0.5 \left[1 + \tanh \left(\lambda \frac{C_{0.5} - C_e}{C_e (1 - C_e)} \right) \right] \quad \dots\dots\dots\dots\dots\dots\dots\dots \quad (19)$$

where $C_{0.5}$ = mean air concentration for $f_e = 0.5f$

$C_{0.5} = 0.0593 + 0.07494 \log R$

$$\lambda = 0.4726 \left\{ 1 + (3.6644 - 0.4729 \log R) \left[2.5915 + \log \left(\frac{k_s}{D_H} \right) \right] \right\}$$

A comparison between (19) and the experimental data is presented in Fig. 7. The results are within the accuracy of the data. The general trend is that, for a given average air concentration, the aerated friction factor increases with the Reynolds number toward the nonaerated friction factor. When the Reynolds number increases, the average shear stress increases and the average bubble size decreases. For small bubble sizes the turbulence is less affected by the presence of the bubbles, which may explain the increase of the aerated friction factor toward the nonaerated values when the Reynolds number increases.

The ratio f_e/f is less affected by the roughness. A close scrutiny of the data suggests that, for low air concentration (i.e. $C_e < 0.40$), the ratio f_e/f increases with the relative roughness for a given Reynolds number. But the lack of data for large air concentrations and large roughness prevents a generalization of that trend. For a given air concentration and Reynolds
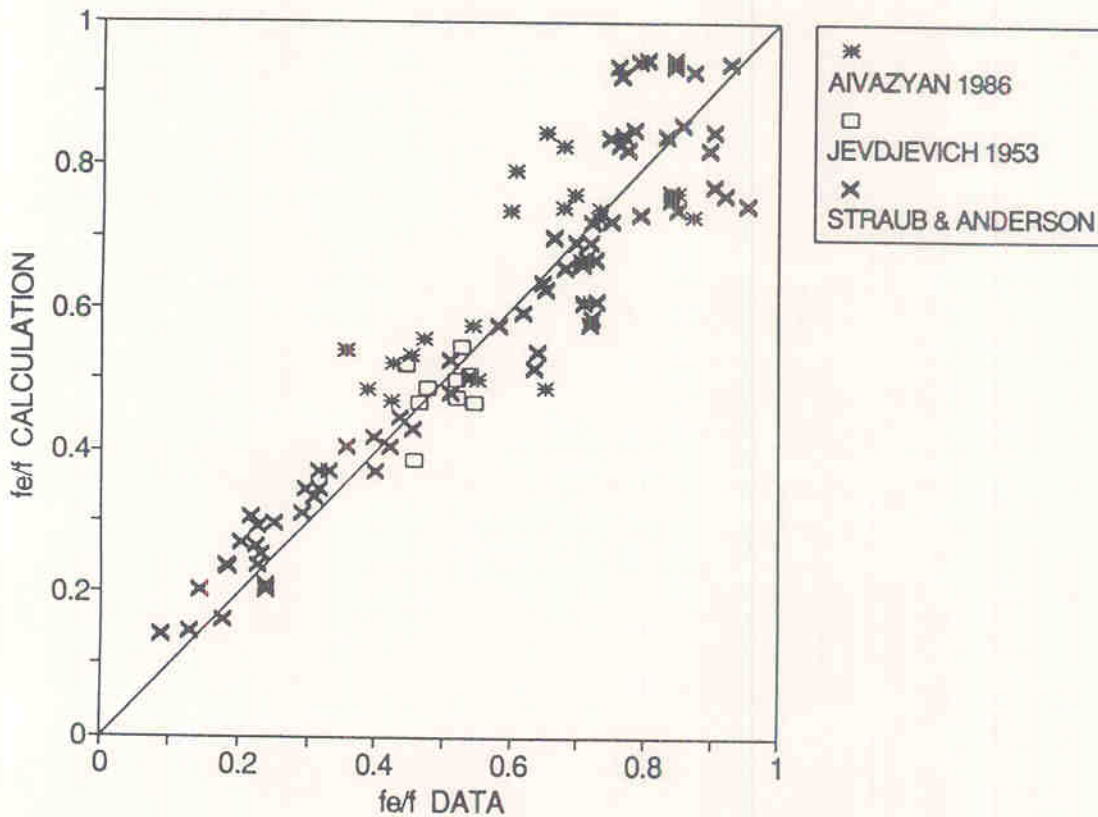

FIG. 7. Comparison of Eq. (19) and Data of Jevdjevich and Levin (1953), Straub and Anderson (1958), and Aivazyan (1986)

number, the shear stress increases with the roughness and the turbulence would be less affected by smaller bubble sizes.

Hartung and Scheuerlein (1970) performed experiments on extremely rough bottom channels (i.e. k_s/D_H in the range of 0.02–0.2) and their results are presented as

$$\frac{f_e}{f} = \frac{1}{[1 - 3.2 \sqrt{f} \log(1 - C_e)]^2} \quad \dotfill (20)$$

where C_e is estimated from (7). This result shows also a reduction of the ratio f_e/f with an increase of air concentration. Further, in fully rough turbulent flows, (20) suggests that the ratio f_e/f is independent of the Reynolds number and decreases with increasing roughness.

Comments

Similar reductions of the friction factor were observed with suspended sediment in water flows. Vanoni (1946) suggested that the effect of the sediment is to reduce the turbulence, and for neutrally buoyant particles, Elata and Ippen (1961) indicated that suspended particles change the structure of the turbulent motion. Observations obtained in sediment flows (Vanoni 1946) and aerated flows (Killen 1968) suggest that the Von Karman universal constant K decreases as the concentration of particles increases. On Aviemore dam, the shape of the velocity distribution implies a value of $K = 0.318$ [(10)]. But Rao and Kobus (1971) showed that the presence of air concentration increases the value of K, while Coleman (1981) indicated that the Karman coefficient does not change with increasing suspended sediment. The complete process is not yet clear, but the writer believes that the interactions between the turbulent shear stress, the velocity distribution, and the air concentration boundary layer next to the channel bottom play a major role in the drag-reduction process. The presence of air bubbles is expected to affect the turbulence, and any change in the Von Karman constant means that the turbulent mixing mechanism has been altered.

The bubble size is an important parameter in the alterations of the turbulence. In aerated flows, the size of the bubbles varies across the flow from large sizes near the free surface ($d_b > 10$ mm) down to small diameters next to the channel bottom ($d_b < 1$ mm) (Cain 1978). In a turbulent shear flow, the mean bubble size is determined by the balance between the capillary force and the inertial force caused by the velocity changes over distances of the order of the bubble diameter. Hinze (1955) showed that the splitting of air bubbles occurs for

$$\frac{\rho_w v^2 d_b}{2\sigma} > W_c \quad \dotfill (21)$$

where v^2 = spatial average value of the square of the velocity differences over a distance equal to d_b; and W_c is a critical Weber number. Experiments showed that W_c is a constant near unity [0.59 in Hinze (1955); 1.26 in Sevik and Park (1973); and 1.02 in Killen (1982)]. A maximum bubble size $(d_b)_c$ can be defined from (21). Assuming that the term v^2 is in the order of magnitude of

$$v^2 \sim \left(\frac{dV}{dy} d_b\right)^2 \quad \dotfill (22)$$

and for a power law velocity distribution, (10), the maximum bubble size is in the order of magnitude of

$$\frac{(d_b)_c}{Y_{90}} \sim \sqrt[3]{2n^2 \frac{W_c}{(\rho_w V_{90}^2 Y_{90}/\sigma)} \left(\frac{y}{Y_{90}}\right)^{2(n-1)/n}} \quad \ldots \ldots \ldots \ldots \ldots \ldots \ldots \ldots \quad (23)$$

where n = exponent of the power law. This simple formulation satisfies the common sense that the maximum bubble size increases with the depth as the shear stress decreases. For Cain's (1978) and Chanson's (1988) flow conditions, with $W_c = 1$ and $n = 6.0$, (23) is presented in Fig. 8. Although (21) was developed for individual bubbles in shear flows, a comparison between the results of (23) and observations of average bubble sizes (Table 3) shows a good agreement.

GRADUALLY VARIED FLOW REGION

Continuity Equation for Air

Downstream of the point of inception, Cain's (1978) data indicate a slow increase of the quantity of air entrained along the spillway. Wood (1985) showed that, for a given mean air concentration, the air concentration distribution has a shape that is close to the equilibrium air concentration distribution. In the gradually varied flow region, assuming a slow variation of the rate of air entrainment, slow variations of the velocity with distance and a hydrostatic pressure distribution, the continuity equation for the air phase, and the energy equation can be solved.

The continuity equation for the air phase yields (Wood 1985)

$$\frac{d}{ds} q_{air} = V_e - C_{mean} u_r \cos \alpha \quad \ldots \ldots \ldots \ldots \ldots \ldots \ldots \ldots \ldots \quad (24)$$
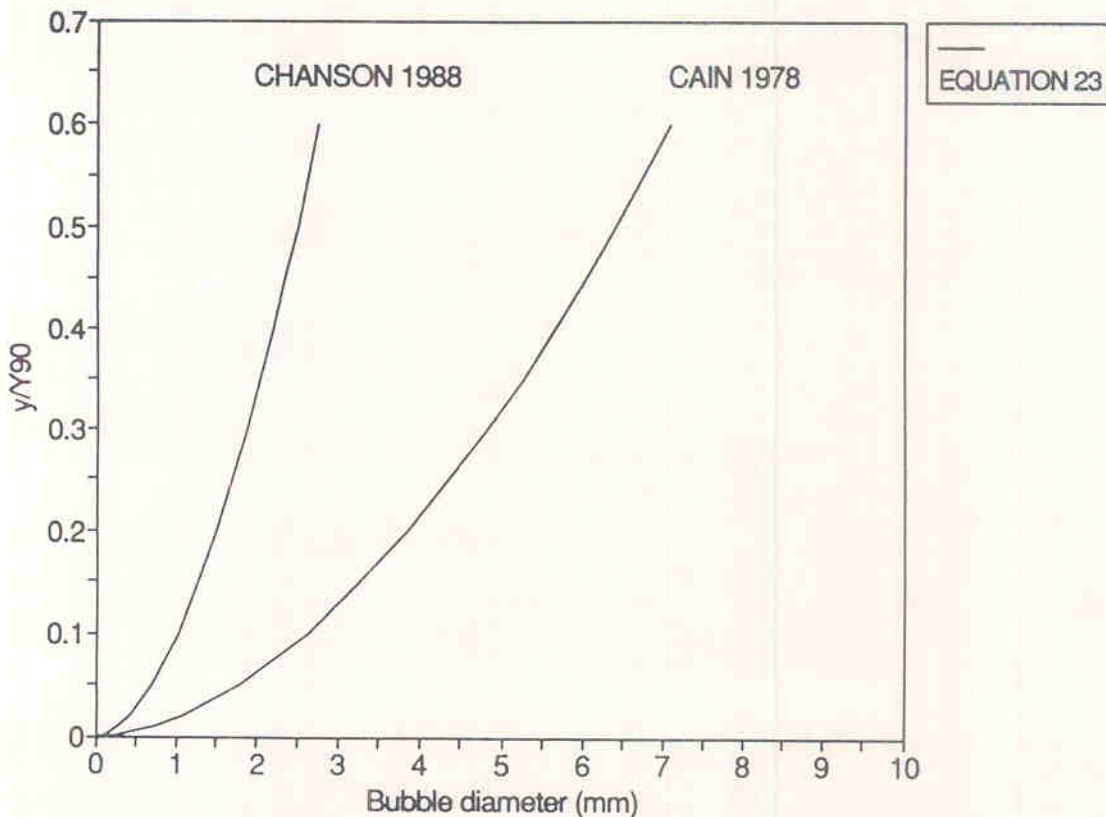

FIG. 8.   Maximum Bubble Size Distribution in Turbulent Shear Flow, Eq. (23)

TABLE 3. Average Bubble Size in Self-Aerated Flows; Observed Values

Experiment (reference) (1)	Slope (degrees) (2)	q_w (m²/s) (3)	V_{90} (m/s) (4)	Y_{90} (m) (5)	d_b (mm) (6)	Comments (7)
Aviemore (Cain 1978)	45.00	2.23; 3.16	20.5; 21.7	0.26; 0.31	3 to 20	Prototype; wide channel
Clyde dam model (Chanson 1988)	52.33	0.20 to 0.40	12.3 to 17.8	0.036 to 0.054	0.3 to 4	Flow downstream of aerator; W = 0.25 m
St. Anthony Falls (Gulliver et al. 1990)	—	0.136 to 0.793	—	—	0.7 to 2.7	Straub and Anderson's experiment; W = 0.457 m

where q_{air} = quantity of air entrained within the flow; u_r = local bubble rise velocity; and V_e = local entrainment velocity. [The quantity of air entrained within the flow and the mean air concentration are related by $q_{air}/q_w = C_{mean}/(1 - C_{mean})$, see discussion by Chanson (1989).] The entrainment velocity characterizes the quantity of air entrained by turbulent eddies close to the free surface. In uniform flow the limit of (24) is

$$0 = (V_e)_e - C_e(u_r)_e \cos \alpha \quad \dots\dots\dots\dots\dots\dots\dots\dots\dots\dots\dots (25)$$

where $(V_e)_e$ and $(u_r)_e$ are the entrainment velocity and rise velocity at equilibrium, in the uniform flow region. Denoting $K_e = V_e/(V_e)_e$ and $K_r = u_r(u_r)_e$, the continuity equation yields

$$\frac{d}{ds} q_{air} = (K_e C_e - K_r C_{mean})(u_r)_e \cos \alpha \quad \dots\dots\dots\dots\dots\dots\dots\dots (26)$$

After transformation the continuity equation for the air phase becomes

$$\frac{d}{ds'} C_{mean} = (1 - C_{mean}) \left[\frac{(u_r)_e d_* \cos \alpha}{q_w} (K_e C_e - K_r C_{mean}) (1 - C_{mean}) \right.$$

$$\left. + \frac{C_{mean}}{W'} \frac{dW'}{ds'} \right] \quad \dots\dots\dots\dots\dots\dots\dots\dots\dots\dots\dots\dots\dots\dots\dots\dots (27)$$

where W = channel width; d_* = flow depth at the origin ($s = 0$); $s' = s/d_*$; and $W' = W/d_*$.

The parameters K_e and K_r are expected to be functions of the turbulence level and bubble size. If the turbulence level and the bubble size distribution vary from the point of inception down to the uniform flow region, the parameters K_e and K_r will be different from unity but will tend toward one in uniform equilibrium flow. For turbulent air-water pipe flows, Wang et al. (1990) showed that the presence of bubbles increases the level of turbulence. For self-aerated flows, the presence of bubbles is thus expected also to increase the level of turbulence, and the entrainment velocity may increase from the point of inception to the uniform region (i.e. $K_e < 1$). Downstream of an aeration device, the high level of turbulence (Chanson

TABLE 4. Entrainment and Rise Velocity Parameters K_e and K_r

K_e (1)	K_r (2)	Application (3)	Comments (4)
>1	<1	Flow downstream of point of inception	Low turbulence and small bubbles
>1	>1	Flow on ski jump	Low turbulence and u_r increases with pressure gradient
=1	=1	Uniform equilibrium flow	—
<1	<1	Flow downstream of an aeration device with steep slope	High turbulence and $C_{mean} < C_e$
<1	=1	Open channel flow in a tunnel spillway; flow downstream of an aeration device with $C_{mean} = C_e$	V_e is reduced by the limited amount of air
<1	>1	Flow downstream of an aeration device with flat slope	High turbulence and $C_{mean} > C_e$

1989) suggests that $K_e > 1$. Also, as the size of the bubbles increases with the mean air concentration and hence the rise velocity, K_r is expected to be less than 1 for $C_{mean} < C_e$. Examples of the writer's expectations for the trend for K_e and K_r are presented in Table 4.

Assuming that the entrainment and rise velocities are the same in gradually varied flow as in uniform flow (i.e. $K_e = K_r = 1$), (27) can be written as

$$\frac{d}{ds'} C_{mean} = (1 - C_{mean}) \left(\frac{u_r d_* \cos \alpha}{q_w} (C_e - C_{mean}) (1 - C_{mean}) \right.$$

$$\left. + \frac{C_{mean}}{W'} \frac{dW'}{ds'} \right) \quad \dots \dots \dots \dots \dots \dots \dots \dots \dots \dots \dots \dots \dots \dots \dots \dots \dots (28)$$

It must be noted that (28) allows the calculations of the average air concentration C_{mean} as a function of the distance along the chute independently of the velocity, roughness, and flow depth. For a channel of constant width, the continuity equation for air becomes the equation obtained by Wood (1985)

$$\frac{d}{ds'} C_{mean} = \frac{u_r d_* \cos \alpha}{q_w} (C_e - C_{mean}) (1 - C_{mean})^2 \quad \dots \dots \dots \dots \dots (29)$$

and for a constant channel slope, the analytical solution is

$$\frac{1}{(1 - C_e)^2} \text{Ln} \left(\frac{1 - C_{mean}}{C_e - C_{mean}} \right) - \frac{1}{(1 - C_e)(1 - C_{mean})} = ks' + K_0 \ .. \ (30)$$

where K_0 and k are

$$K_0 = \frac{1}{1 - C_e} \left[\frac{1}{1 - C_e} \text{Ln} \left(\frac{1 - C_*}{C_e - C_*} \right) - \frac{1}{1 - C_*} \right]$$

$$k = \frac{u_r d_* \cos \alpha}{q_w}$$

in which C_* and $d_* =$ mean air concentration and flow depth at the origin ($s = 0$).

Experimental data on model and prototype self-aerated flows (Straub and Lamb 1956; Isachenko 1965; Rao and Kobus 1971, Cain 1978, Xi 1988) and downstream of an aeration device (Chanson 1988) were used to verify (30). The data provide straight lines with a mean normalized coefficient of correlation of 0.90 (Table 5, column 7). The slope of these lines implies values of the rise velocity u_r in the range of 0.2–41 cm/s (Table 5, column 5). These values of u_r may be interpreted as the average value for each experiment and are plotted as a function of the flow velocity at the start of air entrainment (i.e. $U_w = q_w/d_*$) in Fig. 9.

For self-aerated flows, the flow velocity $U_w = q_w/d_*$ is the point of inception where the flow is nearly uniform and the turbulence quasihomogeneous. Hence the velocity (q_w/d_*) characterizes the turbulence of the flow, and Fig. 9 would suggest that the rise velocity may increase with the turbulence. Even so, this result must be balanced by the effects of the bubble size. The observations of bubble sizes, reported in Table 3, indicate that

TABLE 5. Bubble Rise Velocity: Computed Values

Experiment (1)	Slope (degrees) (2)	q_w (m²/s) (3)	q_w/d_* (m/s) (4)	u_r (m/s) (5)	k_S (mm) (6)	r (7)	Reference (8)
Aviemore dam[a]	45.0	2.23	14.7	0.40	1.0	0.998	Cain (1978)
—	45.0	3.16	16.3	0.39	1.0	0.981	Cain (1978)
Meishan	52.5	0.320	8.3	0.17	0.07	0.995	Xi (1988)
St. Anthony Falls	30.0	0.396	7.4	0.11	0.05	0.988	Straub and Lamb (1956)
Isachenko	21.25	0.15	4.56	0.039	0.1	0.966	Isachenko (1965)
Isachenko	21.25	0.25	5.47	0.033	0.1	0.991	Isachenko (1965)
Isachenko	21.25	0.40	6.47	0.046	0.1	0.983	Isachenko (1965)
Isachenko	21.25	0.60	7.48	0.047	0.1	0.994	Isachenko (1965)
Isachenko	21.25	0.90	8.65	0.043	0.1	0.844	Isachenko (1965)
Isachenko	21.25	0.25	4.85	0.016	3.0	0.682	Isachenko (1965)
Isachenko	21.25	0.40	5.74	0.053	3.0	0.989	Isachenko (1965)
Isachenko	21.25	0.60	6.63	0.069	3.0	0.991	Isachenko (1965)
Isachenko	21.25	0.90	7.66	0.076	3.0	0.991	Isachenko (1965)
Isachenko	21.25	0.25	4.71	0.056	7.0	0.903	Isachenko (1965)
Isachenko	21.25	0.40	5.57	0.061	7.0	0.945	Isachenko (1965)
Isachenko	21.25	0.60	6.43	0.069	7.0	0.903	Isachenko (1965)
Isachenko	21.25	0.90	7.44	0.082	7.0	0.928	Isachenko (1965)
Rao and Kobus	31.98	0.095	4.1	0.003	0.91	0.339	Rao and Kobus (1971)
Clyde dam model[b]	52.33	0.212	8.2	0.11	0.1	0.985	Chanson (1988)
Clyde dam model	52.33	0.396	12.0	0.16	0.1	0.567	Chanson (1988)
Clyde dam model	52.33	0.345	10.5	0.10	0.1	0.714	Chanson (1988)
Clyde dam model	52.33	0.304	9.2	0.048	0.1	0.639	Chanson (1988)
Clyde dam model	52.33	0.273	8.3	0.049	0.1	0.867	Chanson (1988)
Clyde dam model	52.33	0.210	6.4	0.044	0.1	0.977	Chanson (1988)
Clyde dam model	52.33	0.429	6.4	0.011	0.1	0.685	Chanson (1988)

[a]Self-aerated flow.
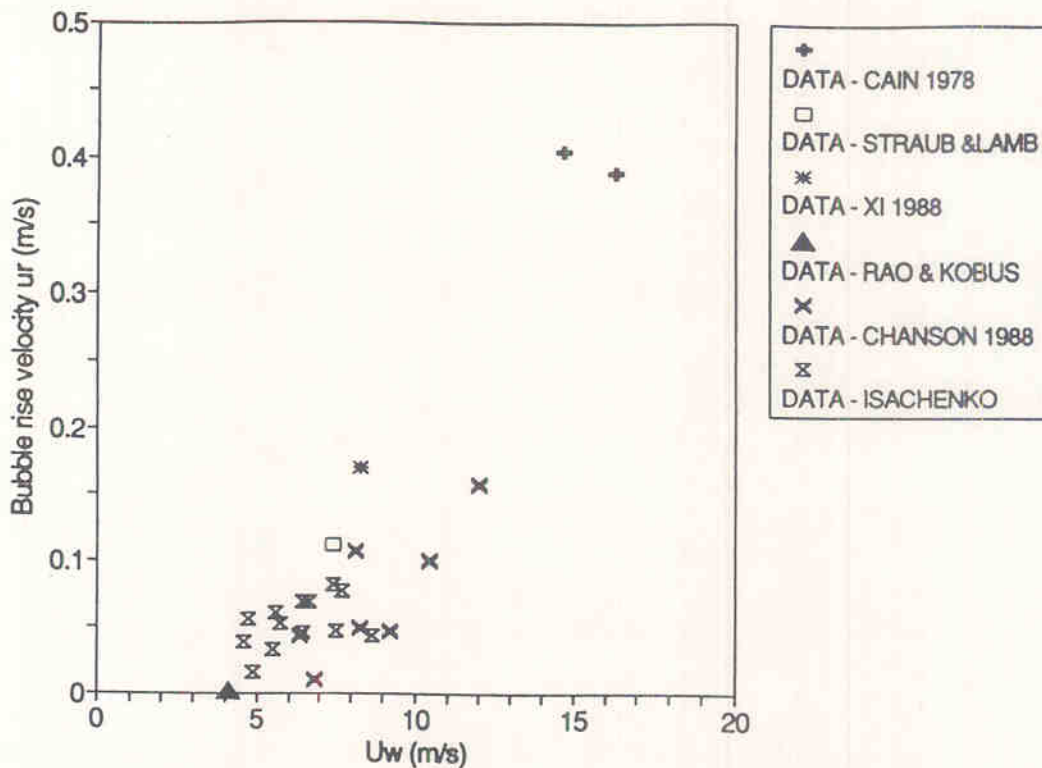[b]Flow downstream of an aeration device.

FIG. 9. Bubble Rise Velocity u_r Estimated from Eq. (30) as Function of Flow Velocity at Start of Self-Aeration $U_w = q_w/d_*$

the largest values of u_r, presented in Fig. 9, were obtained with large bubble sizes (i.e. Cain 1978).

Energy Equation

In the gradually varied flow region, assuming a quasihydrostatic pressure distribution and slow variations of the velocity, the energy equation yields (Wood 1985; Chanson 1989)

$$
\frac{d}{ds'} d' = \frac{\sin \alpha \left(1 + d' \dfrac{d\alpha}{ds'} \right) - S_f + E \dfrac{d'}{W'} \dfrac{F_*^2}{d'^3} \dfrac{dW'}{ds'}}{\cos \alpha - E \dfrac{F_*^2}{d'^3}} \quad \dots \dots \dots \dots \dots (31)
$$

where E = kinetic energy correction parameter, (14) and (16); $d' = d/d_*$, $F_* = q_w/\sqrt{gd_*^3}$; and S_f is the friction slope for aerated flow defined as

$$
S_f = \frac{q_w^2 f_e}{8gd^2} \left(\frac{4}{D_H} \right)
$$

where f_e = local value of the aerated friction factor. The slow increase of flow aeration, observed on both prototype and model, suggests that the friction factor f_e and the energy parameter E can be computed as in uniform flow using the local value of C_{mean}.

Comments

Eqs. (27) and (31) provide two simultaneous differential equations in terms of the mean air concentration and the flow depth, and these equations can be solved with a simple explicit numerical scheme. The knowledge of C_{mean} and d at any point along the chute enables the calculation of Y_{90} in (4); V_{90}, in (12); the integration constants B' and $G' \cos \alpha$; the air concentration distribution, in (8); and the velocity distribution in (10).

It must be emphasized that the calculations depend on the assumed rise velocity u_r. Further, (27) depends also on the assumed coefficients K_e and K_r. At the present time, little information is available on these parameters. As a first approximation it is convenient to use $K_e = K_r = 1$, but these parameters may also be determined empirically from existing experiments as described next.

APPLICATION

Eqs. (29) and (31) were used to reproduce air entrainment on a prototype spillway (Aviemore) and on a large model (Meishan Hydraulics Lab.). Fig. 10 presents a comparison between calculations and data for Cain's (1978) and Xi's (1988) experiments, where L = distance from the point of inception and d_* = flow depth at the point of inception—measured by Cain (1978) at Aviemore dam and computed for Xi's (1988) experiment using Wood's (1985) formula. The rise velocity was obtained from Table 5 and the roughness heights were taken as k_s = 1 mm (Cain 1978) and k_s = 0.03 mm (Xi 1988). In Cain (1978), $\alpha = 45°$; $q_w = 2.16$ m²/s; $d_* = 0.152$ m; $u_r = 0.40$ m/s. In Xi (1988), $\alpha = 52.5°$; $q_w = 0.32$ m²/s; $d_* = 0.039$ m; $u_r = 0.17$ m/s. In each case, the agreement between the data and the analytical results is good.
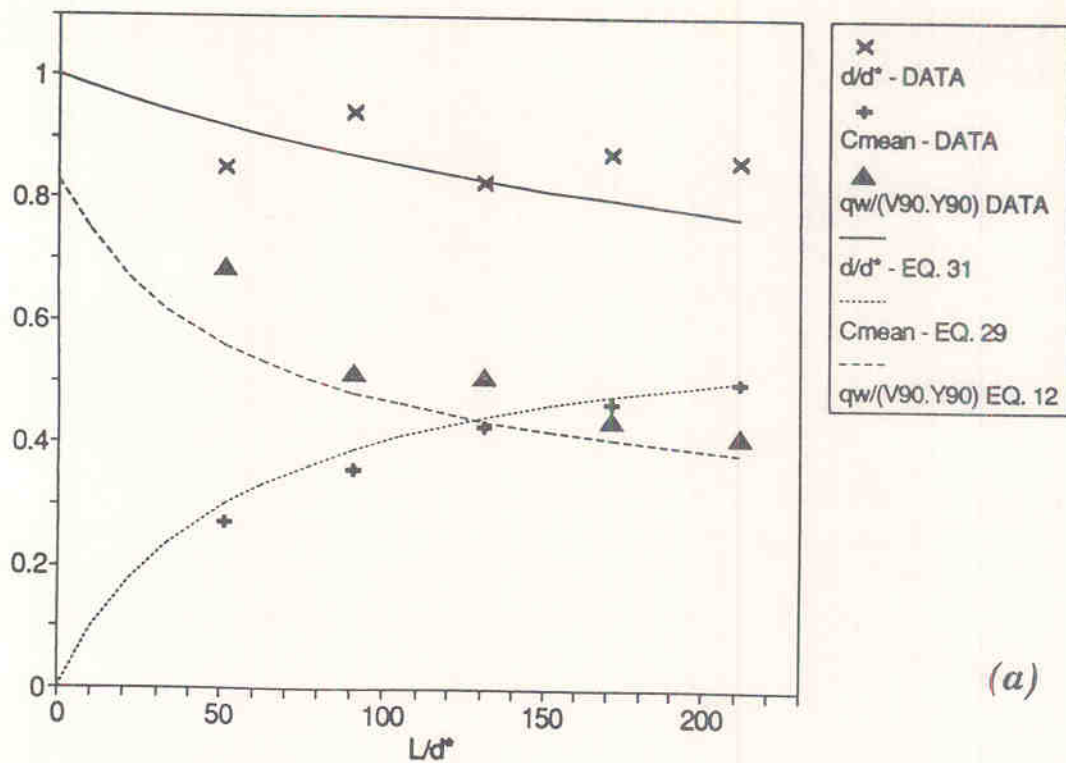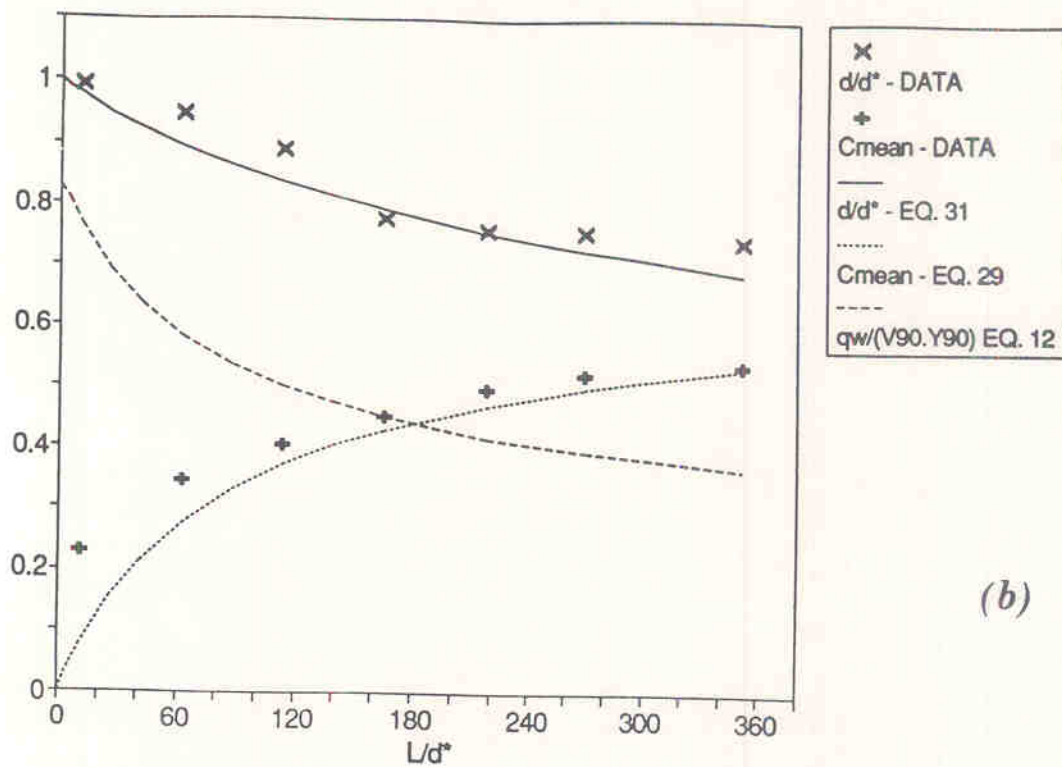
FIG. 10. Self-Aerated Flow Calculations: (a) Cain (1978); (b) Xi (1988)

Application to Tunnel Spillway Flow—Grande-Dixence

Volkart and Rutschmann (1984) performed air concentration measurements in a tunnel spillway of rectangular cross section ($W = 0.8$ m). Using (29), their data suggest computed rise velocities $u_r = 0.023$ m/s and 0.005 m/s for $q_w = 2.75$ m²/s and 5.5 m²/s. These results are not consistent with those obtained in Table 5. Indeed, in a tunnel spillway, the amount of air available above the flow is limited. Further, as the air flow above the water is accelerated, the air pressure will decrease. The entrainment velocity (and

hence K_e) is expected to decrease along the tunnel spillway as the air flow above the water surface is accelerated and as air is entrained within the air-water flow. The buoyancy force is not affected because the pressure gradient across the flow remains quasihydrostatic and the bubble rise velocity may be assumed constant, $u_r = (u_r)_e$.

Fig. 11 shows a comparison between the experimental data obtained by Volkart and Rutschmann (1984) and (27) and (31) as a function of the distance L along the spillway from the intake in which $\alpha = 31°$ and $34.5°$ and $q_w = 2.75$ m²/s. The calculations were done assuming $k_s = 0.1$ mm (steel lining); $K_r = 1$; the coefficient K_e was selected by trial-and-error, decreasing from 0.6 down to 0.5; and the rise velocity $(u_r)_e$ was taken as that computed for Xi's (1988) experiments (i.e. $u_r = 0.17$ m/s) on a flume of similar size and flow velocity.

CONCLUSION

In uniform aerated flows, a complete flow description can be obtained as a function of the channel slope, the water discharge, and the nonaerated friction factor. From the spillway geometry and the discharge, the main flow parameters (i.e. C_e, d, f_e, V_{90}) and the air concentration and velocity distributions can be computed. Comparisons were made with experimental data obtained on model and prototype for slopes in the range 7.5° to 75°. It is believed that the interactions between the shear stress, the air concentration boundary layer, and the velocity distribution next to the channel surface might explain the drag reduction process. But further experimental work is required to obtain a better understanding of the drag reduction mechanisms in self-aerated flows.

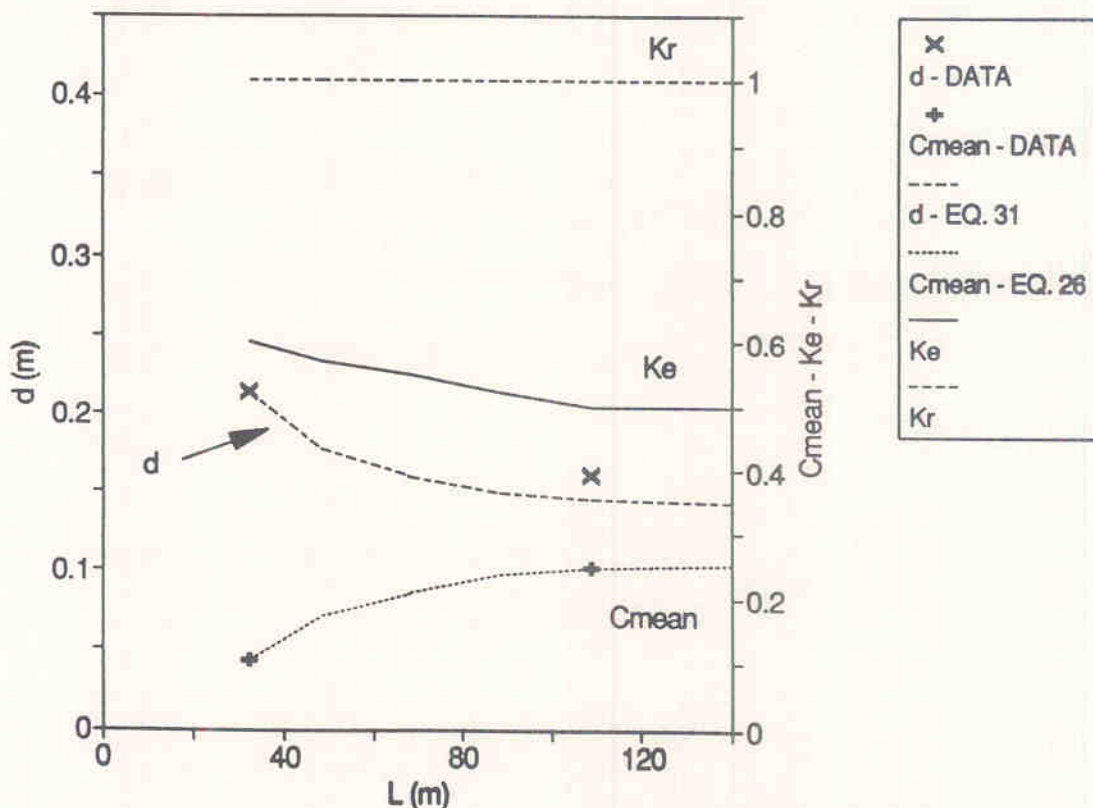In the gradually varied flow region, the continuity equation for air and

FIG. 11. Air Entrainment on Grande-Dixence Tunnel Spillway (Volkart and Rutschmann 1984)

238

the energy equation provides two simultaneous differential equations in terms of the average air concentration and the flow depth. Predictions of self-aeration will, however, depend upon the estimation of the rise velocity, the entrainment velocity, and the non-aerated friction factor. At the present time, insufficient data are available and additional work on the turbulence parameters and bubble sizes is required.

A first analysis of air entrainment in tunnel spillway was developed. The uniform flow conditions are expected to be different from those obtained in chutes. They are a function of the boundary conditions, that is, the geometry of the tunnel, the water flow rate, and the initial air intake geometry.

ACKNOWLEDGMENTS

APPENDIX I. CORRELATIONS BETWEEN RATIO f_e/f, AIR CONCENTRATION, REYNOLDS NUMBER AND ROUGHNESS

The writer investigated the effect of the Reynolds number and roughness on the ratio f_e/f, using the data of Jevdjevich and Levin (1953), Straub and Anderson (1958) and Aivazyan (1987).

First, the writer analyzed the data neglecting the effects of the Reynolds number and relative roughness, and found that the ratio f_e/f may be estimated as

$$\frac{f_e}{f} = 0.5 \left[1 + \tanh \left(0.70 \frac{0.490 - C_e}{C_e(1 - C_e)} \right) \right] \quad \dots \dots \dots (32)$$

with a correlation of $r = 0.898$ (for 104 data points).

For engineering applications, a simple correlation between the ratio f_e/f, the mean air concentration C_{mean}, and the Reynolds number R is

$$\frac{f_e}{f} = 0.307 + 0.1446 \log R - 1.40 \cdot C_{\text{mean}} \quad \dots \dots \dots (33)$$

for $C_{\text{mean}} > 0.25$ and $2 \cdot 10^5 < R < 4 \cdot 10^7$, with a correlation of $r = 0.913$. A more general correlation that works well at the limits is

$$\frac{f_e}{f} = 0.5 \left[1 + \tanh \left(0.7 \frac{C_{0.5} - C_{\text{mean}}}{C_{\text{mean}}(1 - C_{\text{mean}})} \right) \right] \quad \dots \dots \dots (34)$$

where $\tanh(x) = [\exp(x) - \exp(-x)]/[\exp(x) + \exp(-x)]$; and $C_{0.5} =$ mean air concentration for $f_e = 0.5f$

$$C_{0.5} = 0.1032857 \log R - 0.1378571 \quad \dots \dots \dots (35)$$

Eq. (34) was established for Reynolds numbers in the range of $2 \cdot 10^5$ to $4 \cdot 10^7$, and the normalized coefficient of correlation is $r = 0.914$. A more sophisticated correlation for the relationship $f_e/f = \phi(C_{\text{mean}}, R, k_s/D_H)$ that takes into account the influence of the roughness is

$$\frac{f_e}{f} = 0.5 \left[1 + \tanh \left(\lambda \frac{C_{0.5} - C_{mean}}{C_{mean}(1 - C_{mean})} \right) \right] \quad \ldots\ldots\ldots\ldots\ldots\ldots \quad (36)$$

where

$$C_{0.5} = 0.0593 + 0.07494 \log R \quad \ldots\ldots\ldots\ldots\ldots\ldots\ldots\ldots \quad (37)$$

$$\lambda = 0.4726 \left\{ 1 + (3.6644 - 0.4729 \log R) \left[2.5915 + \log \left(\frac{k_S}{D_H} \right) \right] \right\} \quad (38)$$

with a correlation of $r = 0.920$.

APPENDIX II. REFERENCES

Ackers, P., and Priestley, S. J. (1985). "Self-aerated flow down a chute spillway." *Proc., 2nd Int. Conf. on the Hydr. of Floods and Flood Control*, British Hydraulics Research Association, Fluid Engineering, Cambridge, England, 1–16.

Aivazyan, O. M. (1987). "Stabilized aeration on chutes." *Hydrotech. Constr.*, Plenum Publ., 713–722.

Cain, P. (1978). "Measurements within self-aerated flow on a large spillway." *Res. Rep. No. 78-18*, Univ. of Canterbury, Canterbury, New Zealand.

Cain, P., and Wood, I. R. (1981). "Measurements of self-aerated flow on a spillway." *J. Hydr. Div.*, ASCE, 107(11), 1425–1444.

Chanson, H. (1988). "Study of air entrainment and aeration devices on spillway model." *Res. Rep. No. 88-8*, Univ. of Canterbury, Canterbury, New Zealand.

Chanson, H. (1989). "Flow downstream of an aerator—aerator spacing." *J. Hydr. Res.*, 27(4), 519–536.

Chen, C. L. (1990). "Unified theory on power laws for flow resistance." *J. Hydr. Engrg.*, ASCE, 117(3), 371–389.

Coleman, N. L. (1981). "Velocity profiles with suspended sediment." *J. Hydr. Res.*, 19(3), 211–229.

Comolet, R. (1979). "Vitesse d'ascension d'une bulle de gaz isolée dans un liquide peu visqueux." (The terminal velocity of a gas bubble in a liquid of very low viscosity). *Journal de Mécanique Appliquée*, 3(2), 145–171, (in French).

Elata, C., and Ippen, A. T. (1961). "The dynamics of open channel flow with suspensions of neutrally buoyant particles." *Rep. No. 45*, Hydrodynamic Lab., Massachusetts Institute of Technology, Cambridge, Mass.

Ervine, D. A., and Falvey, H. T. (1987). "Behaviour of turbulent water jets in the atmosphere and in plunge pools." *Proc., Institution of Civil Engineers*, Part 2, 83, 295–314.

Falvey, H. T. (1980). "Air-water flow in hydraulic structures." *USBR Engrg. Monograph*, 41, Denver, Colo.

Falvey, H. T. (1990). "Cavitation in chutes and spillways." *USBR Engrg. Monograph*, 42, Denver, Colo.

Gulliver, J. S., Thene, J. R., and Rindels, A. J. (1990). "Indexing gas transfer in self-aerated flows." *J. Envir. Engrg.*, ASCE, 116(3), 503–523.

Hartung, F., and Scheuerlein, H. (1970). "Design of overflow rockfill dams." *Proc., 10th ICOLD Cong.*, Montréal, Canada, 36(35), 587–598.

Hino, M. (1961). "On the mechanism of self-aerated flow on steep slope channels. Applications of the statistical theory of turbulence." *Proc., 9th IAHR Cong.*, Dubrovnick, Yugoslavia, 123–132.

Hinze, J. O. (1955). "Fundamentals of the hydrodynamic mechanism of splitting in dispersion processes." *J. of AIChE*, 1(3), 289–295.

Isachenko, N. B. (1965). "Effect of relative roughness of spillway surface on degrees of free-surface flow aeration." *Izv. VNIIG*, 78, 350–357 (in Russian).

Jevdjevich, V., and Levin, L. (1953). "Entrainment of air in flowing water and technical problems connected with it." *Proc., 5th IAHR Cong.*, Minneapolis, Minn., 439–454.

Keulegan, G. H., and Patterson, G. W. (1940). "A criterion for instability of flow in steep channels." *Trans., Am. Geophysical Union, Part II*, 21, July, 594–596.

Killen, J. M. (1968). "The surface characteristics of self-aerated flow in steep channels." *PhD thesis*, Univ. of Minnesota, Minneapolis, Minn.

Killen, J. M. (1982). "Maximum stable bubble size and associated noise spectra in a turbulent boundary layer." *Proc., Cavitation and Polyphase Flow Forum*, ASME, 1–3.

Knauss, J. (1979). "Computation of maximum discharge at overflow rockfill dams (a comparison of different model test results)." *Proc., 13th ICOLD Congress*, New Delhi, India, 50(9), 143–159.

May, R. W. P. (1987). "Cavitation in hydraulic structures: occurrence and prevention." *Hydraulics Res. Rep., No. SR 79*, Wallingford Hydr. Res. Lab. Wallingford, UK.

Rao, N. S. G., and Rajaratnam, N. (1961). "On the inception of air entrainment in open channel flows." *Proc., 9th IAHR Cong.*, Dubrovnick, Yugoslavia, 9–12.

Rao, N. S. L., and Kobus, H. E. (1971). "Characteristics of self-aerated free-surface flows." *Water and Waste Water: Current Research and Practice*, 10, Eric Schmidt Verlag, Berlin, Germany.

Sevik, M., and Park, S. H. (1973). "The splitting of drops and bubbles by turbulent fluid flow." *J. Fluids Engrg.*, 95(Mar.) 53–60.

Straub, L. G., and Anderson, A. G. (1958). "Experiments on self-aerated flow in open channels." *J. of Hydr. Div.*, ASCE, 84(7), 1890-1–1890-35.

Straub, L. G., and Lamb, O. P. (1956). "Studies of air entrainment in open-channel flows." *Trans.*, ASCE, 121, 30–44.

Vanoni, V. A. (1946). "Transportation of suspended sediment in water." *Trans.*, ASCE, 111, 67–133.

Volkart, P. (1980). "The mechanism of air bubble entrainment in self-aerated flow." *Int. J. Multiphase Flow*, 6, 411–423.

Volkart, P., and Rutschmann, P. (1984). "Rapid flow in spillway chutes with and without deflectors—a model-prototype comparison." *Proc., Symp. on scale effects in modelling hydr. Struct.*, IAHR, Esslingen, Germany, paper 4.5.

Wang, S. K., Lee, S. J., Jones, O. C., and Lahey, R. T. (1990). "Statistical analysis of turbulent two-phase pipe flow." *J. Fluids Engrg.*, ASME, 112(Mar.), 89–95.

Wilhelms, S. C., and Gulliver, J. S. (1989). "Self-aerating spillway flow." *Proc., Nat. Conf. Hydr. Engrg.*, ASCE, 881–886.

Wood, I. R. (1983). "Uniform region of self-aerated flow." *J. Hyd. Engrg.*, ASCE, 109(3), 447–461.

Wood, I. R. (1984). "Air entrainment in high speed flows." *Proc., Symp. on Scale Effects in modelling Hydraulic Structures*, IAHR, Esslingen, Germany, paper 4.1.

Wood, I. R. (1985). "Air water flows." *Proc., 21st IAHR Cong.*, Melbourne, Australia, 18–29.

Xi, R. (1988). "Characteristics of self-aerated flow on steep chutes." *Proc., Int. Symp. on Hydr. for High Dams*, IAHR, Beijing, China, 68–75.

APPENDIX III.   NOTATION

The following symbols are used in this paper:

B' = integration constant of equilibrium air concentration distribution;

C = air concentration defined as volume of air per unit volume;

C_e = depth-averaged equilibrium air concentration (mean air concentration of uniform flow);

C_{mean} = depth-averaged mean air concentration defined as $(1 - C_{mean})Y_{90} = d$;

C_* = mean air concentration at start of gradually varied flow region;

$C_{0.5}$ = mean air concentration for $f_e = 0.5^* f$;

241

D_H = hydraulic diameter (m) defined as $D_H = 4$ Area/Wetted Perimeter $= 4Wd/(W + 2d)$;

d = characteristic flow depth (m);

d_b = air bubble diameter (m);

d_* = characteristic flow depth (m) at start of gradually varied flow region;

d' = dimensionless characteristic flow depth $d' = d/d_*$;

$(d_b)_c$ = maximum bubble diameter in shear flows;

E = kinetic energy correction parameter;

F_* = Froude number at start of gradually varied flow region $F_* = q_w/\sqrt{gd_*^3}$;

f = friction factor of nonaerated flow;

f_e = friction factor of aerated flow;

G' = integration constant of equilibrium air concentration distribution;

g = gravity constant (m/s^2);

K = Von Karman universal constant;

K_e = ratio of the entrainment velocity over equilibrium entrainment velocity $K_e = V_e/(V_e)_e$;

K_r = ratio of local rise velocity over equilibrium rise velocity $K_r = u_r/(u_r)_e$;

k_s = equivalent uniform sand roughness (m);

L = distance along spillway (m);

M = momentum correction parameter;

n = exponent of velocity power law;

q = discharge per unit width (m^2/s);

r = normalized coefficient of correlation;

R = Reynolds number defined as $R = \rho_w U_w D_h/\mu_w$;

S_f = friction slope;

s = curvilinear coordinate (m);

s' = dimensionless curvilinear coordinate: $s' = s/d_*$;

U_w = average water velocity (m/s) defined as $U_w = q_w/d$;

u_r = bubble rise velocity (m/s);

$(u_r)_e$ = bubble rise velocity in uniform equilibrium flow region (m/s);

V = velocity (m/s);

V_e = entrainment velocity (m/s);

$(V_e)_e$ = entrainment velocity in equilibrium flow region (m/s);

V_{90} = characteristic velocity at Y_{90} (m/s);

v' = root mean square of lateral component of turbulent velocity (m/s);

v^2 = spatial average value of square of velocity differences over distance equal to d_b(m^2/s^2);

W = channel width (m);

W_c = critical Weber number characterizing bubble splitting;

W' = dimensionless channel width $W' = W/d_*$;

Y_{90} = characteristic depth (m) where air concentration is 90%;

Y_{98} = characteristic depth (m) where air concentration is 98%;

y = distance from bottom measured perpendicular to spillway surface (m);

y' = dimensionless depth $y' = y/Y_{90}$;

α = spillway slope;

δ_{ab} = thickness (m) of the air concentration boundary layer;

μ = dynamic viscosity (Ns/m^2);
ρ = density (kg/m^3); and
σ = surface tension between air and water (N/m).

Subscripts
air = air flow;
e = equilibrium uniform aerated flow; and
w = water flow.